LETTERS

Seismogenic lavas and explosive eruption forecasting

Y. Lavallée[1], P. G. Meredith[2], D. B. Dingwell[1], K.-U. Hess[1], J. Wassermann[1], B. Cordonnier[1], A. Gerik[1,3] & J. H. Kruhl[3]

Volcanic dome-building episodes commonly exhibit acceleration in both effusive discharge rate and seismicity before explosive eruptions[1]. This should enable the application of material failure forecasting methods to eruption forecasting[2,3]. To date, such methods have been based exclusively on the seismicity of the country rock[4]. It is clear, however, that the rheology and deformation rate of the lava ultimately dictate eruption style[5]. The highly crystalline lavas involved in these eruptions are pseudoplastic fluids that exhibit a strong component of shear thinning as their deformation accelerates across the ductile to brittle transition[6]. Thus, understanding the nature of the ductile–brittle transition in dome lavas may well hold the key to an accurate description of dome growth and stability. Here we present the results of rheological experiments with continuous microseismic monitoring, which reveal that dome lavas are seismogenic and that the character of the seismicity changes markedly across the ductile–brittle transition until complete brittle failure occurs at high strain rates. We conclude that magma seismicity, combined with failure forecasting methods, could potentially be applied successfully to dome-building eruptions for volcanic forecasting.

Arc volcanoes commonly exhibit cycles of dome growth and collapse, leading sometimes to catastrophic explosions. Increasingly, these volcanoes are routinely monitored by multi-parameter (geophysical and geochemical) systems that provide a basis in practice for hazard management and forecasting of upcoming eruptions[1]. Fortunately for the monitoring process, precursory signals of volcanic unrest are common and numerous; yet their origins remain to be deciphered and properly characterized in a mechanistic way. In particular, volcanic eruptions generate various types of seismic signals, including continuous tremor, and it is within the complexities of their waveforms that the description of the responsible internal processes (for example, fluid oscillation, melt migration and fracturing) is likely to be found[7–11]. Although many doubts remain as to the exact nature of volcano-seismic source mechanisms, it is nevertheless commonly accepted that brittle failure along the conduit margin can play a major role[12]. To date, volcanic eruption forecasting models, such as the material failure forecast method (FFM), assume that the seismicity originates from fracturing of the volcanic edifice (and not from the magma)[3,4]. Recent fieldwork on eroded, shallow conduits has uncovered abundant evidence of a more complex magma rheology. In particular, structural and textural evidence have revealed the common existence of seismogenic fault zones in which multiple cycles of rupture, slip and healing have occurred in the magmas owing to strain rate variations across the glass transition[13,14]. Numerical models have further elucidated this shearing-induced fragmentation along the conduit walls; nevertheless, accurate modelling clearly awaits better rheological and seismological constraints[15,16].

Ultimately it is the competition between the strain rate and the relaxation timescale of a melt that dictates whether the eruption will proceed effusively or explosively[5]. Classically, a pure, single-phase melt behaves as a newtonian fluid at low strain rate, but as the deformation speeds up to near the relaxation timescale of the melt structure, the melt becomes non-newtonian. Viscous heating and microcracking ensue[17,18]. In nature, dome lavas inevitably contain variable amount of crystals and bubbles, yet the rheological influence of these features remains obscure[19]. Recent experimental and theoretical studies have helped in defining a realistic view of their non-newtonian behaviour[6,20]. Nevertheless their complex mechanical state, involving components of fluid and solid behaviours, denies us a complete constitutive relationship to date. Essentially, three effects have been recognized as the strain rate (or stress) is increased[6]. (1) An instantaneous viscosity decrease, recoverable upon stress release, defines multiphase lavas as pseudoplastic fluids with a strong component of shear thinning. As the strain rate is further increased, the viscosity becomes strain dependent; a delayed decrease in viscosity is accompanied by (2) viscous heating and (3) audible cracking. This late cracking of lavas, as it embraces the brittle regime, may hold the key to forecasting lava dome eruptions.

The experimental generation of cracks has been studied extensively in the field of rock mechanics[21–23]. Acoustic emissions generated by microcrack growth are used to track the development of macroscopic failure, as their temporal, spatial and size distribution follow a power law akin to that applicable to earthquakes[23]. Acoustic emission events are high-frequency strain waves analogous to low-frequency seismic waves in nature[22]. Yet, acoustic emission has seldom been used to characterize deformation of lavas, even though it has been proposed to provide ''a sensitive procedure for monitoring the nature of creep deformation''[24]. The viscoelastic deformation described in our previous work is comparable to creep deformation[6]. Here we use acoustic emission for the first time (to our knowledge) to characterize the acoustic character of the non-newtonian regime of dome lavas across the ductile–brittle transition—from onset at low strain rate to failure at high strain rate—and to evaluate the failure prediction capability of the FFM.

The experimental arrangement for this investigation couples two now well-established techniques (see Supplementary Information). First, a well-calibrated, high-load, high-temperature uniaxial press was used to study the effects of stress and strain rate on the apparent viscosity of lavas from Colima (Mexico) and Bezymianny (Russia) volcanoes. Second, a fast acoustic-emission monitoring system was close-coupled to the press, and used to record acoustic-emission output simultaneously and continuously during each deformation experiment. Experiments were performed under stresses of 1–40 MPa and temperatures of 940–980 °C, that is, under the pressure–temperature conditions of dome-building eruptions.

Viscosity profiles for multiphase lavas deforming under successively increasing increments of stress have been described recently[6]. Here we extend that work to include the associated acoustic-emission energy released by microcracking during deformation (Fig. 1). Multiphase melt deformation under low stress (8 MPa) is typically characterized by a strong elasticity and thus a viscosity that increases

[1]Department of Earth and Environmental Sciences, Ludwig-Maximilians University, 80333 Munich, Germany. [2]Department of Earth Sciences, University College London, Gower Street, London WC1E 6BT, UK. [3]Faculty of Civil and Geodetic Engineering, Technische Universität München, 80333 Munich, Germany.

at a decreasing rate until it stabilizes at a high, constant value (Fig. 1a). At this low stress, no viscous heating is generated and the temperature remains constant (Fig. 1b). A moderate number of acoustic-emission hits is recorded during the viscosity increase, but with time the acoustic-emission rate decreases to close to zero as viscosity stabilizes. As the acoustic-emission events are generally of low amplitude, the cumulative acoustic-emission energy also remains low (Fig. 1c). At intermediate stress (16 MPa), the viscosity is often observed to remain relatively constant over the duration of the deformation, and viscous heating sometimes increases the temperature (Fig. 1a, b). Under this regime, the acoustic-emission energy rate also remains essentially constant (Fig. 1c) but with occasional higher energy signals. Finally, at high stress (24 MPa), the viscosity decreases markedly during deformation (Fig. 1a). This extreme regime is characterized by 1.6 °C of viscous heating and an accelerating output of acoustic-emission energy (Fig. 1b, c). Overall, the increase in acoustic-emission energy with increasing stress is due to an increase in both the number of hits and the individual hit amplitude (compare earthquake magnitude). This is, in turn, manifested in a decrease of the seismic *b*-value from >3.5 to as low as <1.5 in some cases (the *b*-value is the slope of the amplitude–frequency relationship; see Supplementary Information). This observation implies a change from more distributed small-scale cracking at lower stresses to more localized larger-scale cracking at higher stresses.

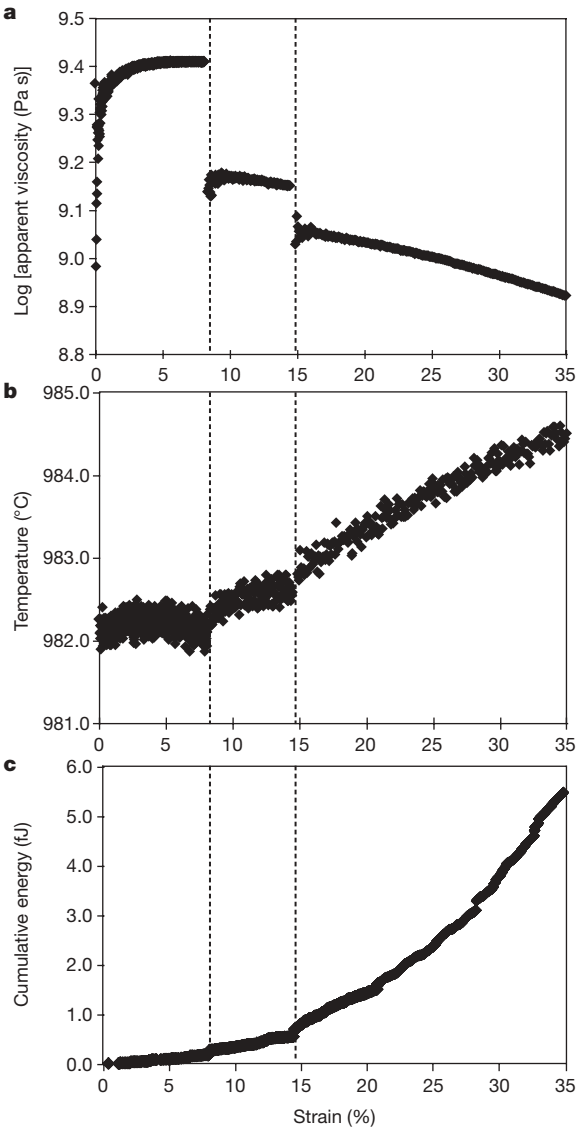

Figure 1 | Experimental results for successive deformation of a Colima lava melt at 8, 16 and 24 MPa. In each panel, the vertical dashed lines show when the pressure was changed; left line, 8 to 16 MPa; right line, 16 to 24 MPa. **a**, The apparent viscosity profile shows the instantaneous decrease associated with each stress increment. This is the origin of the non-newtonian behaviour. **b**, The internal melt temperature shows an increase associated with minor viscous heating at high stress. **c**, The cumulative acoustic-emission energy output is minor and constant at low to moderate stress, and increases exponentially at high stress (1 fJ = 10^{-15} J).

Suspension rheology involves cracking throughout the spectrum. The deformation is nearly aseismic at strain rates below $10^{-4}\,s^{-1}$. Then, the rates of acoustic-emission output increases nonlinearly with increasing strain rate and accelerates as failure is approached (Fig. 2). The presence of crystals within a melt lowers the strain rate corresponding to the onset of the ductile–brittle transition in these multiphase magmas. Textural analysis of deformed samples indicates that cracking generally initiates in plagioclase crystals. At high strain rate, experiments revealed the alignment of crystals and the development of large-scale cracks (also reflected in the decrease of seismic *b*-value). Complementary quantitative analyses of fabrics developed in Colima and Bezymianny samples using the fabric analysis software AMOCADO[25] revealed an increase in the anisotropy—represented by the fitted ellipse's axial ratio—of the groundmass pattern by ~29% upon 33% strain (Fig. 3). The anisotropy of the crystal pattern, however, decreased by 19%. These observations suggest that during deformation, elongate crystals become broken into more equant fragments (lowering the crystal anisotropy) while the fragments from the original crystals align themselves perpendicularly to the applied stress to ease flow migration of the interstitial melt (increasing the overall anisotropy).

Given our observation that multiphase lavas behave in a brittle fashion at high strain rate, we have chosen to test whether crack growth and macroscopic failure of a multiphase melt at high strain rate is comparable to rock failure. The FFM relies on the production rate of precursory phenomena (for example, seismicity rate, acoustic-emission rate, seismic energy release), and correlating their accelerations to the likeliness of failure—in this case, of an eruption—via the equation

$$\frac{d^2\Omega}{dt^2} = A\left(\frac{d\Omega}{dt}\right)^{\alpha} \quad (1)$$

where $d^2\Omega/dt^2$ and $d\Omega/dt$ are the acceleration and rate of the phenomenon being monitored, and A and α are empirically determined parameters[2,3,26–28]. More explicitly, α is expected to evolve from 1 to 2 before an eruption[27]. A recent description of the fracturing time series that arise from random energy fluctuations within a finite volume subject to a constant remote stress proposed that the peaks in event

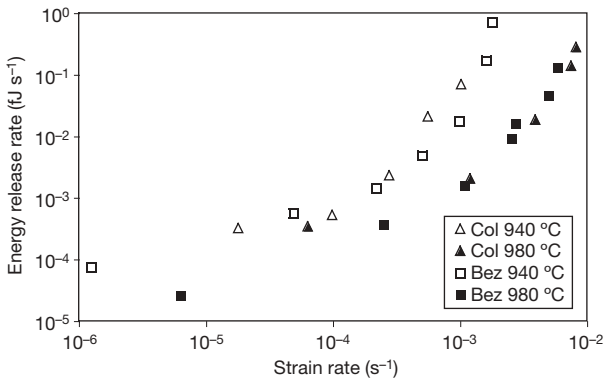

Figure 2 | Acoustic-emission energy release rates for Colima and Bezymianny lavas at different strain rates. Although the crystallinities of Colima (Col; ~55% crystals) and Bezymianny (Bez; ~80% crystals) melt samples were significantly different, the behaviours of both melts were very similar at a given temperature. It is rather the temperature that may serve to attenuate acoustic emission.

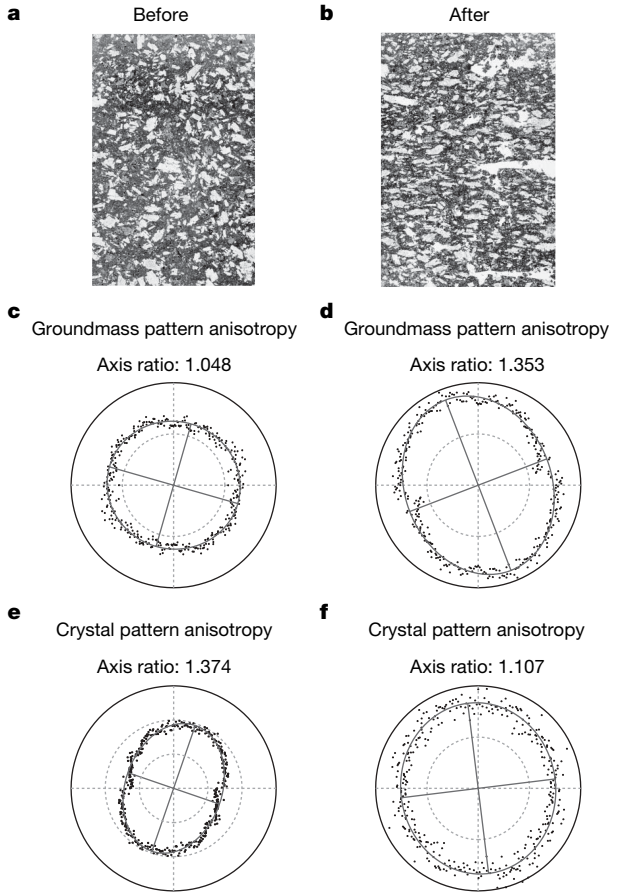

Figure 3 | Anisotropy changes associated with deformation. These images and anisotropy analyses show the results of an experiment on Colima lava at 940 °C under a pressure of 40 MPa. **a**, **b**, Photographs of thin sections before the experiment (**a**), and after the experiment (**b**; the applied stress was parallel to the long axis of the thin section). Both thin sections were prepared along the same plane in the original rock sample. Photograph **b** shows a clear alignment of the crystals perpendicular to the applied stress. **c**, **d**, The anisotropy of the groundmass increased by 39% when comparing the axis ratios of the fitted ellipse before the experiment (**c**), and after the experiment (**d**). **e**, **f**, In contrast, the anisotropy of the crystal pattern decreased by 19%, when comparing the results before (**e**) and after (**f**). These anisotropies are visualized by direction versus size coefficient distribution plots. The coefficients are calculated from segment length distributions received from scanlines superposed on the analysed fabric. Each ring is equivalent to a count of 500 units (**c**), 1,000 units (**d**), 1,250 units (**e**), and 50 units (**f**); see ref. 25 for details.

rate (rather than all seismic events) predict best the path to failure, and that $\alpha = 2$ when approaching failure[2]. The equation can thus be simplified to:

$$\frac{1}{\mathrm{d}\Omega/\mathrm{d}t} = A(t_\mathrm{f} - t) \qquad (2)$$

where t_f is the expected time-to-failure. As the acceleration increases before failure, the extrapolation of the inverse rate to zero should provide the time-to-failure. Although empirically derived from the field of rock mechanics, this approach appears to provide a good representation of precursory accelerations preceding natural eruptions[28]—especially when the acceleration of energy released is used[29]. However, the predictions yielded by the model remain uncertain until shortly before an eruption, and thus an improved treatment must unfortunately await better rheological and seismological constraints[29].

Our deformation experiments at very high strain rates on Colima lavas were characterized by an accelerating acoustic-emission event rate and energy rate until complete failure soon thereafter. We can

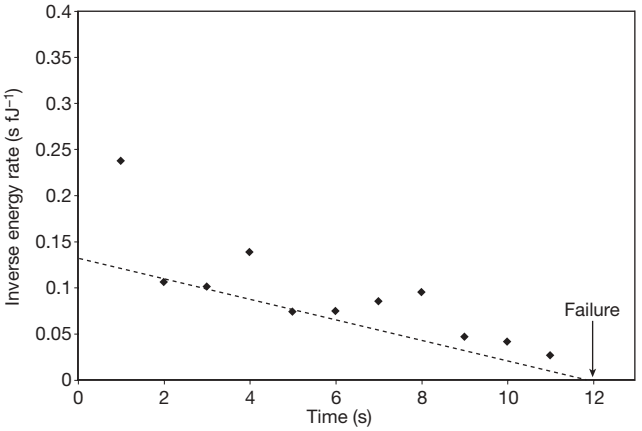

Figure 4 | Application of the FFM to a Colima lava. Experiment at 940 °C deformed under 40 MPa (strain rate of $7 \times 10^{-3}\,\mathrm{s}^{-1}$). The FFM prediction was based on the extrapolation of peak energy rates (lower values on this inverse scale), following ref. 2. Extrapolation of peak energy rates after 4 s of deformation (dashed line) well predicts the time of complete failure (arrow).

therefore retrieve a data distribution analogous to acoustic emission measured for rocks before failure by simply inverting the acoustic-emission rate as shown in Fig. 4. Extrapolations of the peak energy rate data points after four seconds indeed yield a very accurate prediction of the macroscopic failure of lava, which occurred after 12 seconds. Although the test cannot be used to model more accurate α values at this point, it strongly suggests that the choice of an exponent equalling two and the use of peak energy values are appropriate for the forecasts of lava dome eruption induced by shear strain. An earlier attempt to use the acceleration of seismic energy release to forecast two volcanic eruptions at Colima has shown that the method only became reasonably accurate shortly before the eruption[28]. That study further specifies that such forecasting models "require that the medium be considered as a closed-continuum system". Under such conditions, our work raises the possibility of accurate early predictions. We attribute the difficulty of using the FFM in real time during volcanic crises to the use of seismic data that may not all originate from a common process. For instance, stick-slip motion along fault planes in the upper conduit (for example, Mount St Helens[30]) would alter the seismic signals derived from shear-induced fragmentation at greater depth. Such a signal distinction is an essential prerequisite for future forecasting attempts. The present findings indicate that runaway growth of the strain rate and seismic energy release rates before volcanic eruption is likely to be the result of lava crossing the ductile–brittle transition as a result of increasing strain rate.

The present work may have an effect on eruption forecast modelling. This series of rheological and acoustic tests has been able to expose the strongly seismogenic character of multiphase lavas across the ductile–brittle transitional field. At strain rates below $10^{-4}\,\mathrm{s}^{-1}$, lavas are nearly aseismic. In contrast, high-strain-rate experiments clearly reveal an accelerating rate of seismic energy release and a localization of the cracking until complete failure around $10^{-3}\,\mathrm{s}^{-1}$ (at 940 °C) and $10^{-2}\,\mathrm{s}^{-1}$ (at 980 °C). Energy rate acceleration before failure at high strain rates directly supports the application of FFM to dome-building eruptions. We conclude that it may be beneficial to test this technique in areas of volcanic unrest.

Received 15 November 2007; accepted 2 April 2008.

1. Sparks, R. S. J. Forecasting volcanic eruptions. *Earth Planet. Sci. Lett.* **210**, 1–15 (2003).
2. Kilburn, C. R. J. Multiscale fracturing as a key to forecasting volcanic eruptions. *J. Volcanol. Geotherm. Res.* **125**, 271–289 (2003).
3. Voight, B. A method for prediction of volcanic eruptions. *Nature* **332**, 125–130 (1988).
4. Voight, B. A relation to describe rate-dependent material failure. *Science* **243**, 200–203 (1989).
5. Dingwell, D. B. Volcanic dilemma: Flow or blow? *Science* **273**, 1054–1055 (1996).

6. Lavallée, Y., Hess, K. U., Cordonnier, B. & Dingwell, D. B. A non-Newtonian rheological law for highly-crystalline dome lavas. *Geology* **35,** 843–846 (2007).
7. McNutt, S. R. Volcanic seismology. *Annu. Rev. Earth Planet. Sci.* **33,** 461–491 (2005).
8. Neuberg, J., Luckett, R., Baptie, B. & Olsen, K. Models of tremor and low-frequency earthquake swarms on Montserrat. *J. Volcanol. Geotherm. Res.* **101,** 83–104 (2000).
9. Neuberg, J. Characteristics and causes of shallow seismicity in andesite volcanoes. *Phil. Trans. R. Soc. Lond. A* **358,** 1533–1546 (2000).
10. Chouet, B. A. Long-period volcano seismicity: Its source and use in eruption forecasting. *Nature* **380,** 309–316 (1996).
11. Harrington, R. M. & Brodsky, E. E. Volcanic hybrid earthquakes that are brittle-failure events. *Geophys. Res. Lett.* **34,** doi:10.1029/2006GL028714 (2007).
12. Neuberg, J. W. *et al.* The trigger mechanism of low-frequency earthquakes on Montserrat. *J. Volcanol. Geotherm. Res.* **153,** 37–50 (2006).
13. Tuffen, H. & Dingwell, D. B. Fault textures in volcanic conduits: Evidence for seismic trigger mechanisms during silicic eruptions. *Bull. Volcanol.* **67,** 370–387 (2005).
14. Tuffen, H., Dingwell, D. B. & Pinkerton, H. Repeated fracture and healing of silicic magma generate flow banding and earthquakes? *Geology* **31,** 1089–1092 (2003).
15. Gonnermann, H. M. & Manga, M. Explosive volcanism may not be an inevitable consequence of magma fragmentation. *Nature* **426,** 432–435 (2003).
16. Papale, P. Strain-induced magma fragmentation in explosive eruptions. *Nature* **397,** 425–428 (1999).
17. Hess, K. U., Cordonnier, B., Lavalée, Y. & Dingwell, D. B. Viscous heating in rhyolite: an in situ determination. *Earth Planet. Sci. Lett.* (in the press).
18. Webb, S. L. & Dingwell, D. B. The onset of non-Newtonian rheology of silicate melts — a fiber elongation study. *Phys. Chem. Miner.* **17,** 125–132 (1990).
19. Petford, N. Rheology of granitic magmas during ascent and emplacement. *Annu. Rev. Earth Planet. Sci.* **31,** 399–427 (2003).
20. Costa, A. Viscosity of high crystal content melts: Dependence on solid fraction. *Geophys. Res. Lett.* **32,** doi:10.1029/2005GL024303 (2005).
21. Prikryl, R., Lokajicek, T., Li, C. & Rudajev, V. Acoustic emission characteristics and failure of uniaxially stressed granitic rocks: The effect of rock fabric. *Rock Mech. Rock Eng.* **36,** 255–270 (2003).
22. Dobson, D. P., Meredith, P. G. & Boon, S. A. Detection and analysis of microseismicity in multi anvil experiments. *Phys. Earth Planet. Inter.* **143–44,** 337–346 (2004).
23. Ojala, I. O., Main, I. G. & Ngwenya, B. T. Strain rate and temperature dependence of Omori law scaling constants of AE data: Implications for earthquake foreshock-aftershock sequences. *Geophys. Res. Lett.* **31,** doi:10.1029/2004GL020781 (2004).
24. Chmelik, F. *et al.* An evaluation of the creep characteristics of an AZ91 magnesium alloy composite using acoustic emission. *Mater. Sci. Eng. A* **338,** 1–7 (2002).
25. Gerik, A. & Kruhl, J. H. Towards automated pattern quantification: Time-efficient assessment of anisotropy of 2D patterns with AMOCADO. *Comput. Geosci.* (in the press).
26. Tokarev, P. On a possibility of forecasting of Bezymianny volcano eruptions according to seismic data. *Bull. Volcanol.* **26,** 379–386 (1963).
27. Cornelius, R. R. & Voight, B. Graphical and PC-software analysis of volcano eruption precursors according to the materials failure forecast method (FFM). *J. Volcanol. Geotherm. Res.* **64,** 295–320 (1995).
28. De la Cruz-Reyna, S. & Reyes-Davila, G. A. A model to describe precursory material-failure phenomena: Applications to short-term forecasting at Colima volcano, Mexico. *Bull. Volcanol.* **63,** 297–308 (2001).
29. Smith, R., Kilburn, C. R. J. & Sammonds, P. R. Rock fracture as a precursor to lava dome eruptions at Mount St Helens from June 1980 to October 1986. *Bull. Volcanol.* **69,** 681–693 (2007).
30. Iverson, R. M. *et al.* Dynamics of seismogenic volcanic extrusion at Mount St. Helens in 2004–05. *Geology* **444,** 439–443 (2006).

Supplementary Information is linked to the online version of the paper at www.nature.com/nature.

Acknowledgements We thank O. Spieler for collecting the samples, K. T. Fehr, S. Bernstein and J. Pawlowski for assistance during microprobe analyses and M. Sieber for technical assistance. This is publication no. GEOTECH-315 of the research and development programme GEOTECHNOLOGIEN.

Author Contributions Y.L., P.G.M. and B.C. performed the acoustic-emission experiments; Y.L. analysed the data under the complementary supervisions of D.B.D., K.-U.H. and J.W.; and A.G. and J.H.K. performed the quantitative pattern analyses.

Author Information Reprints and permissions information is available at www.nature.com/reprints. Correspondence and requests for materials should be addressed to Y.L. (lavallee@min.uni-muenchen.de).